

 Open access • Journal Article • DOI:10.1007/BF02814892

Creep behavior of electron-beam-melted rhenium — Source link

Walter R. Witzke, Peter L. Raffo

Institutions: Glenn Research Center

Published on: 01 Apr 1971

Topics: Rhenium, Creep, Activation energy, Powder metallurgy and Metal powder

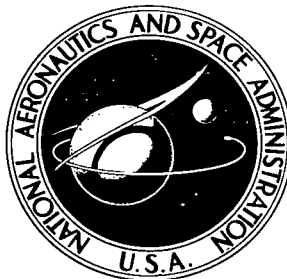
Related papers:

- [Influence of tungsten and rhenium concentration on creep properties of a second generation superalloy](#)
- [Strengthening Factors and Phase Relation in Ni-Cr-W Alloys Developed for Nuclear Steelmaking](#)
- [Effect of nitrogen high temperature plasma based ion implantation on the creep behavior of Ti-6Al-4V alloy](#)
- [Creep behaviors and microstructure evolution of Mg-5Y-2Nd-3Sm-0.5Zr alloys](#)
- [High-temperature creep of a CoNiCrAlY bond coat alloy](#)

Share this paper:    

View more about this paper here: <https://typeset.io/papers/creep-behavior-of-electron-beam-melted-rhenium-1i4r7ngwyj>

NASA TECHNICAL NOTE



NASA TN D-6291

C1

NASA TN D-6291

LOAN COPY: RETURN TO
AFWL (DOCUMENTS)
KIRTLAND AFB

0133135



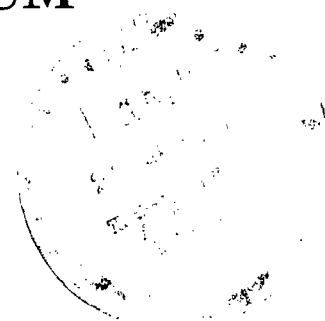
TECH LIBRARY KAFB, NM

CREEP BEHAVIOR OF ELECTRON-BEAM-MELTED RHENIUM

by Walter R. Witzke and Peter L. Raffo

Lewis Research Center

Cleveland, Ohio 44135





0133135

1. Report No. NASA TN D-6291	2. Government Accession No.	3. Recipient's Catalog No.	
4. Title and Subtitle CREEP BEHAVIOR OF ELECTRON-BEAM-MELTED RHENIUM		5. Report Date April 1971	6. Performing Organization Code
7. Author(s) Walter R. Witzke and Peter L. Raffo		8. Performing Organization Report No. E-6073	
9. Performing Organization Name and Address Lewis Research Center National Aeronautics and Space Administration Cleveland, Ohio 44135		10. Work Unit No. 129-03	
12. Sponsoring Agency Name and Address National Aeronautics and Space Administration Washington, D.C. 20546		11. Contract or Grant No.	
15. Supplementary Notes		13. Type of Report and Period Covered Technical Note	
16. Abstract Creep deformation in electron-beam-melted polycrystalline rhenium sheet was evaluated at 2200 ⁰ to 4200 ⁰ F (1477 to 2588 K) and 4 to 40 ksi (28 to 276 MN/m ²). Comparisons were made with powder-metallurgy rhenium under similar conditions. Changes in creep-rupture behavior resulting from electron beam melting of rhenium were greater ductility, higher primary creep rate, and longer rupture life, especially at lower temperatures. The activation energy for creep was 72 kcal/mole (301 J/mole) for electron-beam-melted rhenium and 64 kcal/mole (268 J/mole) for powder-metallurgy rhenium.		14. Sponsoring Agency Code	
17. Key Words (Suggested by Author(s)) Rhenium Electron-beam melted Creep Powder metallurgy Rupture life Ductility Activation energy Polycrystalline		18. Distribution Statement Unclassified - unlimited	
19. Security Classif. (of this report) Unclassified	20. Security Classif. (of this page) Unclassified	21. No. of Pages 24	22. Price* \$3.00

CREEP BEHAVIOR OF ELECTRON-BEAM-MELTED RHENIUM

by Walter R. Witzke and Peter L. Raffo

Lewis Research Center

SUMMARY

The creep behavior of electron-beam-melted (EB) polycrystalline rhenium sheet was studied in the temperature range 2200^o to 4200^o F (1477 to 2588 K) under constant load with stresses ranging from 4 to 40 ksi (28 to 276 MN/m²). Comparisons were made with similarly tested powder-metallurgy (PM) rhenium sheet.

The improvements in creep properties derived from electron beam melting of rhenium were greater ductility and longer rupture life, particularly at lower temperatures. Primary creep rates for EB rhenium were higher, but secondary creep rates were comparable to those for PM rhenium. The improved creep and rupture characteristics are attributed to the reduction of voids and impurities by the vacuum melting. The activation energy for creep between 2200^o and 4200^o F (1477 and 2588 K) was 72 kilocalories per mole (301 J/mole) for EB rhenium and 64 kilocalories per mole (268 J/mole) for PM rhenium. The rate-controlling process in this temperature range is associated with dislocation pipe diffusion.

INTRODUCTION

The potential usefulness of rhenium as an aerospace material can be expressed in terms of its refractory character, stiffness, and low-temperature ductility. Rhenium has a hexagonal close-packed crystal structure and a melting point of 5750^o F (3450 K), the second highest of the metals. Its modulus of elasticity at room temperature approximates 67×10⁶ psi (4.6×10⁵ MN/m²) and it has enough ductility to be fabricable at room temperature. Although it is costly and scarce, rhenium and its alloys can be expected to be used in specialized design applications.

The mechanical properties of unalloyed rhenium have not been investigated in as much detail as those of the other refractory metals, tungsten, molybdenum, columbium, and tantalum. Literature reviews of rhenium up to 1960 (refs. 1 and 2) indicate a small amount of data on the tensile and stress-rupture properties of powder-metallurgy wire

as the only information available on the high-temperature properties of rhenium. Since that time, additional mechanical property data, including creep and stress-rupture data on powder-metallurgy sheet at high temperatures, have been reported (refs. 3 to 5).

Because electron beam melting has shown improved properties in other metals due to purification, this vacuum melting process could possibly render improvements in rhenium also. In general, electron-beam-melted materials have been described as having superior ductility to arc-cast or sintered stock (ref. 6).

The objective of the present study was to characterize the high-temperature creep deformation of polycrystalline rhenium sheet rolled from an electron-beam-melted (EB) ingot. Creep rupture, step-load, and step-temperature creep tests were performed in the temperature range 2200° to 4200° F (1477 to 2588 K, 0.43 to $0.75T_m$) at stresses ranging from 4 to 40 ksi (28 to 276 MN/m²). These data are compared with similar test data on commercial powder-metallurgy (PM) rhenium sheet and with previous literature data.

EXPERIMENTAL PROCEDURE

Materials

Commercial rhenium powder having a minus-200 mesh particle size was used in preparing the EB rhenium. The supplier's analysis of the powder is given in table I. PM rhenium sheet 0.040 inch (0.10 cm) thick was obtained commercially and used for comparison testing. A small amount of the PM rhenium sheet was rolled to a thickness of 0.020 inch (0.050 cm).

Melting

In preparation for electron beam melting, 9 pounds (4.1 kg) of rhenium powder were hydrostatically pressed at 30 ksi (208 MN/m²) into a 1.25-inch (3.2-cm) diameter bar and sintered in dry hydrogen at 4000° F (2477 K) for 3 hours. Melting was performed in a commercial 150-kilowatt electron beam furnace previously described in reference 7. The rhenium metal was double melted into a 2-inch (5-cm) diameter mold at a power level of 80 to 100 kilowatts with the chamber pressure maintained at 5×10^{-5} torr. The average Vickers hardness (10-kg load) across the diameter of the double-melted ingot near its top was 225 DPH. Taken in several grains of varying crystallographic orientations, 18 hardness indentations ranged in value from 181 to 270 DPH. This large spread reflects the extreme hardness anisotropy typical of hexagonal close-packed metals.

Fabrication

The fabrication of the EB rhenium ingot was accomplished by first extruding at 3800⁰ F (2366 K) and then by rolling at room temperature with intermediate recrystallization anneals. The extrusion step is unique in rhenium fabrication. Rhenium is seldom worked above room temperature because of embrittlement due to hot-shortness problems. The hot shortness is thought to be due to the melting of a Re₂O₇ oxide normally situated at the grain boundaries (ref. 8). Hot shortness was avoided in the present work by extruding the rhenium in an evacuated and sealed container. Rhenium is also characterized by rapid work hardening. The high extrusion temperature was chosen so that the deformation would occur above the work-hardening temperature range.

Preparations for extrusion involved grinding of the ingot surface, sealing the billet in 0.01-inch (0.025-cm) thick tantalum sheet using gas tungsten-arc (TIG) and EB welding, and canning in powder-metallurgy Mo - 25-weight-percent W alloy. The purpose of the claddings was to prevent the formation of low-melting Re₂O₇ and to facilitate the extrusion.

The clad rhenium was successfully extruded at 3800⁰ F (2366 K) and a reduction ratio of 8:1. The extrusion speed was about 5 inches per second (13 cm/sec) with a breakthrough pressure of 118 ksi (814 MN/m²). Thus, with suitable precautions to avoid hot-short and work-hardening characteristics, the extrusion of rhenium at high temperatures has been shown to be feasible. (This general extrusion procedure was suggested by Dr. Fred J. Rollfinke of Cleveland Refractory Metals, Solon, Ohio.)

The resultant flat bar was ground to remove the cladding. The extruded rhenium was fully recrystallized with an average grain diameter of 66 micrometers. The average Vickers hardness (10-kg load) was 176 DPH.

Room-temperature rolling was required to bring the rhenium to a final 0.020-inch (0.050-cm) thickness. Reductions of 8 to 10 percent were made per rolling pass. Due to the rapid work-hardening rate of rhenium, after each 15 to 20 percent total reduction the sheet was recrystallized by annealing in hydrogen for 5 minutes at 3000⁰ F (1922 K). The final as-rolled sheet was approximately 60 percent recrystallized with an average Vickers hardness (200-g load) of 536 DPH.

Testing

Creep test specimens were cut from EB and PM rhenium sheet materials by electro-spark machining. The specimens were 3.25 inches (8.25 cm) long by 0.63 inch (1.60 cm) wide with a 1.0-inch (2.54-cm) long by 0.25-inch (0.64-cm) wide test section. Prior to testing, all specimens were annealed in a hydrogen atmosphere for 1 hour at 3000⁰ F (1922 K). Both materials were fully recrystallized by the treatment (see fig. 1)

and had average grain diameters of 37 micrometers for the EB rhenium sheet and 47 micrometers for the PM rhenium sheet.

Creep testing was performed in vacuum (10^{-5} to 10^{-7} torr; 10^{-3} to 10^{-5} N/m²) under constant load. Stresses ranged from 4 to 40 ksi (28 to 276 MN/m²) and temperatures ranged from 2200^o to 4200^o F (1477 to 2588 K). Deformation was recorded during the creep tests from load-train displacement measurements. Strains were determined on the basis of this measurement and the assumption that all the creep occurred in the gage length. The minimum creep rates were determined graphically.

The majority of the creep tests consisted of applying a constant load and permitting the material to elongate to rupture. Other tests that were conducted for determining secondary creep rates under varying conditions consisted of changing the load (step loading) or temperature (step temperature) periodically. Step changes were made as the creep rate approached a minimum.

Chemical Analysis

The EB and PM rhenium sheet materials were analyzed to determine impurity contents. A comparison of the emission spectrographic analysis given in table I suggests only small differences in impurity levels between the EB and PM sheet. Both materials were of very high purity, namely >99.99 percent Re. The content levels of most of the metallic and interstitial impurities are unfortunately at or near the present quantitative limits of detection. The values of analyzed impurity content, therefore, may not present a true picture of the differences between the EB and PM rhenium materials. Indirect evidence of the higher purity of the EB-melted rhenium is presented in the sections RESULTS and DISCUSSION.

Metallography

Standard optical microscopy techniques were used in examining the rhenium specimens. The microstructures of the mechanically polished sections were best revealed by etching with Murakami's etchant and through use of polarized light. Grain diameter measurements were made by the line intercept method.

RESULTS

Grain Growth Observations

Indirect evidence of the higher purity of EB-melted rhenium compared to the PM rhenium material was afforded both by the results of annealing studies and observations of the grain size of specimens after creep testing. As shown in figure 2, the powder-metallurgy rhenium sheet was remarkably resistant to grain growth during annealing. Specimens recrystallized at 3000° F (1922 K) showed essentially no grain growth in 1-hour anneals at temperatures as high as 4000° F (2477 K). On the other hand, the EB rhenium exhibited grain growth beginning at approximately 3200° F (2033 K). We believe this difference in grain growth behavior reflects the higher purity of the EB rhenium, since small quantities of impurities can have a pronounced effect on the grain-boundary migration rate (ref. 9).

This difference in grain growth behavior may account for some of the observed differences in creep behavior of the two types of rhenium at temperatures above 3000° F (1922 K), as will be discussed later. Observations made on the unstrained portions of the test specimens indicated that the grain size of the EB rhenium increased during tests at 3000° F (1922 K) and above, while that of the PM rhenium remained constant.

Creep-Rupture Life and Ductility

The results of the creep tests conducted on the EB and PM rhenium sheet are listed in table II and illustrated in figures 3 to 8. Creep curves for both types of rhenium at 2200° , 3000° , and 4000° F (1477, 1922, and 2477 K) are compared in figure 3. The most striking differences in behavior were the much greater rupture ductility and longer rupture life of the EB rhenium at 2000° and 3000° F (1477 and 1922 K) in figures 3(a) and (b), respectively. For example, at 2200° F (1477 K) at a stress of 20 ksi (138 MN/m²), the elongation at rupture for the EB rhenium was 22 percent, while that of the PM rhenium was only 4 percent. The higher ductility of the EB rhenium appears to be responsible for its much longer rupture life, 721 hours as compared to 32.2 hours for the PM rhenium under the previously noted test conditions. These large differences are not attributable to differences in grain size of the two materials, for the grain sizes were very comparable and stable during these lower temperature tests.

At 4000° F (2477 K) (fig. 3(c)), where differences in grain growth behavior might be expected to influence the test results, the difference in rupture life and ductility were much smaller than at the lower temperatures. Under the test conditions illustrated in figure 3(c), there appeared to be a significant effect of specimen thickness on the rupture

life and ductility of the PM rhenium sheet. The 1.0-millimeter-thick sheet appeared to be significantly less ductile and exhibited a shorter rupture life than the 0.5-millimeter sheet. Unfortunately, this variable was not explored in EB rhenium sheet or at test temperatures of 3000⁰ F (1922 K) or lower, so the extent to which a size effect may influence the results at lower temperatures is unknown.

Secondary Creep Behavior

The temperature dependence of the secondary (minimum) creep rate $\dot{\epsilon}$ is shown for EB and PM rhenium in figure 4 for stress σ levels ranging from 4 to 40 ksi (28 to 276 MN/m²). The activation energy for creep Q_c for EB rhenium was determined from this plot to have an average value of 72 kilocalories per mole (301 J/mole) and was relatively independent of stress. The Q_c for the PM rhenium was previously reported by the authors at 64 kilocalories per mole (268 J/mole) (ref. 5). Vandervoort and Barmore have determined Q_c for PM rhenium as 60 kilocalories per mole (251 J/mole) (ref. 4).

A least-squares treatment of the data indicated a stress exponent n of 3.7 for EB rhenium and 3.5 for PM rhenium. These relatively low exponent values are in agreement with the work of Vandervoort and Barmore (ref. 4), who observed a value of 3.4 for PM rhenium. However, a log-log plot of $\dot{\epsilon}$ against σ at constant temperature for the EB rhenium data suggested a possible increase in n to 4.3 above 3400⁰ F (2144 K). Insufficient information was available to determine the validity or possible causes of a higher stress exponent.

Figure 5 shows the stress dependence of the temperature-compensated creep rate $\dot{\epsilon} \exp(Q_c/RT)$ where Q_c for the composite data is 69 kilocalories per mole (289 J/mole). The stress exponent for EB rhenium is 3.6 for almost the entire stress range, whereas for PM rhenium the stress dependency ranges from 2.2 at low stresses to 4.8 above 10 ksi (69 MN/m²). In the high-temperature creep of most pure metals, n is observed between 4 and 6 (ref. 10).

Primary Creep Behavior

Primary creep rates were determined according to the Andrade $t^{1/3}$ law using the expression

$$\epsilon = \beta t^{1/3} + \dot{\epsilon} t$$

where the measured strain ϵ at time t consists of strain components related to the primary creep rate β and the secondary creep rate $\dot{\epsilon}$.

The temperature dependencies of the primary creep rates for EB and PM rhenium are shown in figure 6. Activation energies determined from these plots averaged 87 kilocalories per mole (373 J/mole) for EB rhenium and 78 kilocalories per mole (327 J/mole) for PM rhenium. These values are about 20 percent higher than the activation energies determined for secondary creep. Previous studies have indicated that the activation energy remains relatively constant during primary and secondary creep, provided no change in deformation mode occurs (ref. 10).

The relation between the primary and secondary creep of rhenium was examined. This is shown in figure 7, where β is plotted versus $\dot{\epsilon}$ for the EB and PM rhenium creep-rupture tests. The data for the two materials do not coincide, but the slopes of the least-squares determinations were nearly identical and indicated the relation

$$\beta = k(\dot{\epsilon})^{0.4}$$

The magnitudes of the primary creep rates for EB rhenium were greater than for PM rhenium by a factor slightly less than 3.

Rupture Life Behavior

The effect of creep stress on rupture life at constant temperature is shown by means of a log-log plot in figure 8 for three temperature levels. The slopes of the stress-rupture life data for the various temperatures for each sheet material have been drawn parallel to each other. At 4000^o F (2477 K) the effect of stress for both EB and PM rhenium sheet materials can be described by a single line. However, as the test temperature was decreased, a difference in stress-rupture life behavior of the two materials became more apparent. Although EB rhenium had approximately the same life as PM rhenium at 4000^o F (2477 K), at 3000^o F (1922 K) EB rhenium had about three times the life of PM rhenium, while at 2200^o F (1477 K) EB rhenium lasted over 20 times longer than PM rhenium. The stress for a 100-hour rupture life at 2200^o F (1477 K) was 30 ksi (207 MN/m²) for EB rhenium, almost twice that for PM rhenium.

Rupture data from reference 3 for PM rhenium (lot 1) at 2912^o and 3996^o F (1873 and 2473 K) are also shown in figure 8 for comparison. A difference in stress dependency can be noted. The rhenium materials from this study had a stress dependency coefficient of -4.8 compared to -3.7 for the data from reference 3.

DISCUSSION

Considerable differences have been observed in the properties of electron-beam-melted (EB) rhenium sheet compared to powder-metallurgy (PM) rhenium sheet. Relative to PM rhenium the results of this study have shown that EB rhenium had

- (1) Greater ductility
- (2) Longer rupture life
- (3) Higher primary creep rates
- (4) Similar secondary creep rates
- (5) Grain growth initiating at a much lower temperature

With the essential difference in processing being the additional steps of melting and extruding, it can be assumed that these property differences are mainly due to melting. An accepted consequence of melting refractory metals under good vacuum conditions is the generally increased purity of the product. That this might occur in the electron beam melting of already high-purity rhenium powder compacts was not known. However, as shown in figure 1 the melting was beneficial in preparing a material with relatively few voids. Also indirect evidence suggesting increased purity was noted in the grain growth characteristics of the two materials. The decrease in impurities and voids can reasonably account for the greater ductility (as measured by total elongation) and longer rupture life of EB rhenium.

Void formation during creep testing was observed in both EB and PM rhenium, as shown in figure 9. Voids at the grain boundaries were larger in the PM rhenium at 2 percent elongation, where rupture occurred, than in the EB rhenium at 9 percent elongation, where the test was interrupted.

Tertiary creep has been associated with the development of voids at the grain boundaries (ref. 11). Resnick and Seigle (ref. 12) have shown that the removal of impurities which catalyze void formation during diffusion also decreases the tendency for grain-boundary void formation during creep and thereby significantly improves the stress-rupture life of the material. The existence of voids in the grain boundaries before creep testing probably accounts for the lower strain values observed in PM rhenium prior to tertiary creep, compared to EB rhenium, and thereby serves to reduce rupture life.

Under the same test conditions the secondary creep rates of the two rhenium materials were similar, but, as observed in figure 6, the primary creep rates of the EB rhenium were higher than those for PM rhenium. For a given secondary creep rate, the primary creep rate for EB rhenium was shown in figure 7 to be greater by a factor of 3. This is consistent with the greater ease of dislocation movement that would be expected with increased purity.

The activation energy for creep in pure metals above one-half the absolute melting temperature has been shown in a large number of investigations to be nearly equal to the activation energy for self diffusion (ref. 13). Experimentally determined values of the activation energy for self-diffusion in rhenium are not available, but estimates based on the melting point suggest values ranging from 117 to 131 kilocalories per mole (490 to 548 J/mole). The apparent activation energies for creep determined in this investigation, however, are approximately one-half the estimated values for self-diffusion, indicating the creep behavior of rhenium in this temperature range (0.43 to $0.75T_m$) is not controlled by dislocation climb. As would be expected, the activation energies resulting from this investigation are somewhat higher than those experimentally evaluated for surface diffusion of rhenium (ref. 14), ranging from 48.4 to 53.0 kilocalories per mole (203 to 222 J/mole) depending on crystal orientation.

Vandervoort and Barmore (ref. 4) observed that creep deformation in rhenium took place by dislocation motion within the grain and that no subgrain formation occurred. This ruled out grain boundary and sub-boundary diffusion. In accord with Vandervoort and Barmore's conclusions and with those previously proposed by the authors (ref. 5) the rate-controlling process in the high-temperature creep of rhenium is associated with dislocation pipe diffusion.

SUMMARY OF RESULTS

The creep properties of rhenium sheet prepared from electron-beam-melted and extruded material were compared with sheet prepared by commercial powder-metallurgy methods. The results of this study in the temperature range 0.43 to $0.75T_m$ were as follows:

1. Compared to PM rhenium, EB rhenium had greater ductility (total elongation), longer rupture life, and higher primary creep rates. For example, at 2200° F (1477 K) EB rhenium had 5.5 times the total elongation and 20 times the rupture life exhibited by PM rhenium. These differences decreased as temperature increased. Secondary creep rates were comparable. We believe that the improved creep and rupture properties of EB rhenium can be attributed to the reduction in impurities and voids by vacuum melting.

2. Activation energies for creep between 2200° and 4200° F (1477 and 2588 K) ranged from 72 kilocalories per mole (301 J/mole) for EB rhenium to 64 kilocalories per mole

(268 J/mole) for PM rhenium. The rate-controlling process in this temperature range is associated by the authors with dislocation pipe diffusion.

Lewis Research Center,
National Aeronautics and Space Administration,
Cleveland, Ohio, January 5, 1971,
129-03.

REFERENCES

1. Sims, C. T.; Wyler, E. N.; Gaines, G. B.; and Rosenbaum, D. M.: A Survey of the Literature of Rhenium. Battelle Memorial Inst. (WADC-TR-56 319), June 1956.
2. Gonser, B. W., ed.: Rhenium. Elsevier Publ. Co., 1962.
3. Conway, J. B.; and Flagella, P. N.: Creep-Rupture Data for the Refractory Metals to High Temperatures. Rep. GEMP-685, General Electric Co., Mar. 1969.
4. Vandervoort, R. R.; and Barmore, W. L.: High-Temperature Plastic Deformation of Polycrystalline Rhenium. Trans. AIME, vol. 245, no. 4, Apr. 1969, pp. 825-829.
5. Raffo, Peter L.; and Witzke, Walter R.: Creep of Powder Metallurgy Rhenium at 0.43 to 0.72 T_m . Trans. AIME., vol. 245, no. 4, Apr. 1969, pp. 889-890.
6. Bakish, Robert, ed.: Introduction to Electron Beam Technology. John Wiley & Sons, Inc., 1962.
7. Witzke, Walter R.; Sutherland, Earl C.; and Watson, Gordon, K.: Preliminary Investigation of Melting, Extruding, and Mechanical Properties of Electron-Beam-Melted Tungsten. NASA TN D-1707, 1963.
8. Lebert, G.: Behavior of Rhenium During Hot Working. In Rhenium. B.W. Gonser, ed., Elsevier Publ. Co., 1962, pp. 126-136.
9. Gordon, Paul: Annealing Mechanisms in Deformed Metals. Energetics in Metallurgical Phenomena. Vol. 1. W. M. Mueller, ed., Gordon and Breach Science Publ., 1965, pp. 205-239.
10. Garofalo, Frank: Fundamentals of Creep and Creep-Rupture in Metals. Macmillan Co., 1965.
11. Davies, P. W.; and Evans, R. W.: The Contribution of Voids to the Tertiary Creep of Gold. Acta Met., vol. 13, no. 3, Mar. 1965, pp. 353-361.

12. Resnick, R.; and Seigle, L.: Nucleation of Voids in Metals During Diffusion and Creep. *J. Metals*, vol. 9, no. 1, Jan. 1957, pp. 87-94.
13. Dorn, J. E.: The Spectrum of Activation Energies for Creep. Seminar on Creep and Recovery. ASM, 1957, pp. 225-283.
14. Bettler, Philip C.; and Barnes, George: Field-Emission Studies of Surface Migration for Tungsten, Rhenium, Iridium, and Rhodium. *Surface Sci.*, vol. 10, 1968, pp. 165-176.

TABLE I. - RHENIUM ANALYSES

Impurity element (a)	Impurity content, ppm		
	Commercial powder (supplier analysis)	Commercial powder-metallurgy sheet	Electron-beam-melted sheet
Ac	(b)	----	-----
Al	<1	3	5
Ca	<1	----	-----
Co	----	.2	< .2
Cr	<1	6	3
Cu	<1	----	-----
Fe	8	30	15
Mg	<1	----	-----
Mn	(b)	.5	< 3
Mo	<1	.2	< .2
Na	<1	----	-----
Nb	----	.6	< .2
Ni	<1	2	.7
Si	<1	----	-----
Sn	(b)	----	-----
Ta	----	2	1
Ti	(b)	.3	.2
V	(b)	----	-----
W	(b)	5	< .2
Zr	(b)	1.6	.5
C	59	8	11
N	40	5	4
O	2700	6	8
H	42	----	-----

^aElements other than interstitials determined by emission spectrography.

^bNot detected.

TABLE II. - CREEP PROPERTIES OF UNALLOYED RHENIUM

(a) Powder-metallurgy rhenium sheet

Load stress, σ		Test temperature, T		Primary creep rate, $\dot{\epsilon}_1$, $\text{sec}^{-1/3}$	Secondary creep rate, $\dot{\epsilon}_2$, sec^{-1}	Rupture life, t_R , hr	Total elongation, percent	Average grain diameter, μm , ^a	Nominal sheet thickness, mm
ksi	MN/m ²	°F	K						
4	28	3000	1922	1.64×10^{-4}	1.37×10^{-7}	290	14	68	1
		3200	2033	1.64	2.31	(b)	--	--	.5
		3500	2200	1.64	8.33	(b)	--	41	.5
		3500	2200	4.70	8.41	32.9	18	--	1
		3800	2366	5.04	2.30×10^{-5}	23.3	21	44	.5
		3900	2422	6.32	2.72	11.5	24	57	.5
		4000	2477	7.27	3.69	15.1	24	48	.5
		4000	2477	5.98	2.99	10.5	18	62	1
		4200	2588	7.10	5.87	8.13	20	51	.5
		6	41	2700	1755	7.10×10^{-4}	4.80×10^{-8}	(b)	--
3000	1922			2.22	3.85×10^{-7}	75.1	12	--	1
3000	1922			-----	3.75	(b)	--	--	.5
3200	2033			-----	6.96	(b)	--	--	.5
3500	2200			-----	3.44×10^{-6}	(b)	--	--	.5
3500	2200			4.66	2.36	8.56	12	48	1
3800	2366			-----	1.15×10^{-5}	(b)	--	39	.5
4000	2477			9.76	1.35	1.74	14	--	1
4000	2477			9.01	1.48	2.44	15	56	.5
4200	2588			-----	3.64	.89	22	54	.5
10	69	2500	1644	1.26×10^{-4}	1.29×10^{-7}	108	8	--	1
		2700	1755	2.46	3.00	49.3	8	--	↓
		3000	1922	5.17	1.33×10^{-6}	11.0	10	57	↓
		3000	1922	4.55	1.75	10.3	12	53	↓
		3500	2200	1.37×10^{-3}	1.68×10^{-5}	.90	10	65	↓
15	103	2200	1477	1.33×10^{-4}	6.06×10^{-8}	133	8	--	1
		2500	1644	2.90	4.70×10^{-7}	17.1	6	--	↓
		2700	1755	6.00	1.72×10^{-6}	5.79	8	--	↓
		3000	1922	1.06×10^{-3}	1.25×10^{-5}	.80	8	59	↓
20	138	2200	1477	2.16×10^{-4}	1.91×10^{-7}	32.2	8	--	1
		2500	1644	-----	2.70×10^{-6}	2.72	8	--	1

^aMeasured on unstrained portion of specimen after test.

^bStep-temperature creep test.

TABLE II. - Continued. CREEP PROPERTIES OF UNALLOYED RHENIUM

(b) Electron-beam-melted rhenium sheet

Load stress, σ		Test temperature, T		Primary creep rate, $\dot{\epsilon}_1$, $\text{sec}^{-1/3}$	Secondary creep rate, $\dot{\epsilon}_2$, sec^{-1}	Rupture life, t_R , hr	Total elongation, percent	Average grain diameter, μm , ^a	Nominal sheet thickness, mm		
ksi	MN/m ²	°F	K								
4	28	3000	1922	-----	1.12×10^{-7}	(c)	----	---	0.5 ↓		
		3000	1922	-----	1.44	(b)	----	---			
		3000	1922	-----	1.66	(d)	(4)	75			
		3200	2033	-----	4.28×10^{-4}	1.38	164	11		122	
		3200	2033	-----	-----	2.10	(b)	----		---	
		3200	2033	-----	-----	2.40	(b)	----		---	
		3400	2144	-----	-----	8.41	(b)	----		204	
		3500	2200	-----	-----	5.96	2.36	106		12	299
				↓	↓	8.99	3.62	68.5		17	219
						-----	3.63	(b)		----	---
						-----	4.34	(c)		----	---
						-----	5.41	(b)		----	---
				3800	2366	-----	1.15×10^{-6}	(b)		----	264
				3800	2366	-----	2.54	(b)		----	---
				3800	2366	-----	2.58	(b)		----	---
				4000	2477	-----	1.61×10^{-3}	2.86		16.9	29
		4000	2477	-----	-----	4.09	(b)	----	264		
		4200	2588	-----	1.35×10^{-5}	2.81	28	284			
6	41	2800	1810	-----	1.27×10^{-7}	(b)	----	---	0.5 ↓		
		3000	1922	-----	3.30	(c)	----	---			
		3200	2033	-----	6.18	(b)	----	---			
		3400	2144	-----	-----	4.00×10^{-6}	(b, c)	----		---	
		3500	2200	-----	-----	1.74	14.6	17		212	
		3500	2200	-----	-----	2.56	(c)	----		---	
		3500	2200	-----	-----	2.78	(b)	----		---	
		3800	2366	-----	-----	1.62×10^{-5}	(b)	----		---	
		3900	2422	-----	-----	2.85×10^{-3}	1.20	(d)		(10)	199
		4000	2477	-----	-----	3.74	3.26	1.37		25	370

^aMeasured on unstrained portion of specimen after test.

^bStep-temperature creep test.

^cStep-load creep test.

^dSpecimen broke in grip during creep-rupture test.

TABLE II. - Concluded. CREEP PROPERTIES OF UNALLOYED RHENIUM

(b) Concluded. Electron-beam-melted rhenium sheet

Load stress, σ		Test temperature, T		Primary creep rate, $\dot{\epsilon}_1$, $\text{sec}^{-1/3}$	Secondary creep rate, $\dot{\epsilon}_2$, sec^{-1}	Rupture life, t_R , hr	Total elongation, percent	Average grain diameter, μm , ^a	Nominal sheet thickness, mm
ksi	MN/m ²	^o F	K						
8	55	2500	1644	-----	4.95×10^{-8}	(b)	-----	----	0.5 ↓
			1644	-----	5.81	(b)	-----	----	
		2700	1755	-----	1.74×10^{-7}	(b)	-----	----	
			1810	-----	1.88	(b)	-----	----	
		3000	1922	-----	6.10	(b)	-----	----	
			1922	-----	1.08×10^{-6}	(c)	-----	----	
		3200	2033	-----	2.92	(b)	-----	----	
			2200	-----	7.70	(c)	-----	----	
		3500	2200	-----	1.73×10^{-5}	(b)	-----	----	
			2366	3.82×10^{-3}	3.09	1.33	22	168	
		2366	4.47	4.14	1.53	21	183		
4000	-----	8.51	.43	21	303				
10	69	2500	1644	3.50×10^{-4}	8.95×10^{-8}	304	14	61	0.5 ↓
			1922	-----	2.59×10^{-6}	12.7	14	39	
		1922	-----	2.25	(c)	-----	----		
		3500	3.53×10^{-3}	1.72×10^{-5}	2.61	20	185		
		2200	-----	3.09	(c)	-----	276		
15	103	2200	1477	2.85×10^{-4}	2.99×10^{-8}	^e >>350	(>>4)	45	0.5 ↓
			1922	2.76×10^{-3}	7.24×10^{-6}	5.10	21	63	
		1922	-----	9.29	(c)	-----	----		
		3500	6.93	9.25×10^{-5}	.48	24	118		
20	138	2200	1477	5.40×10^{-4}	5.59×10^{-8}	721	26	29	0.5 ↓
			1644	1.48×10^{-3}	1.60×10^{-6}	(d)	(9)	42	
		1922	-----	3.87×10^{-5}	(c)	-----	103	.5	
40	276	2200	1477	-----	1.74×10^{-6}	24.5	20	----	0.5

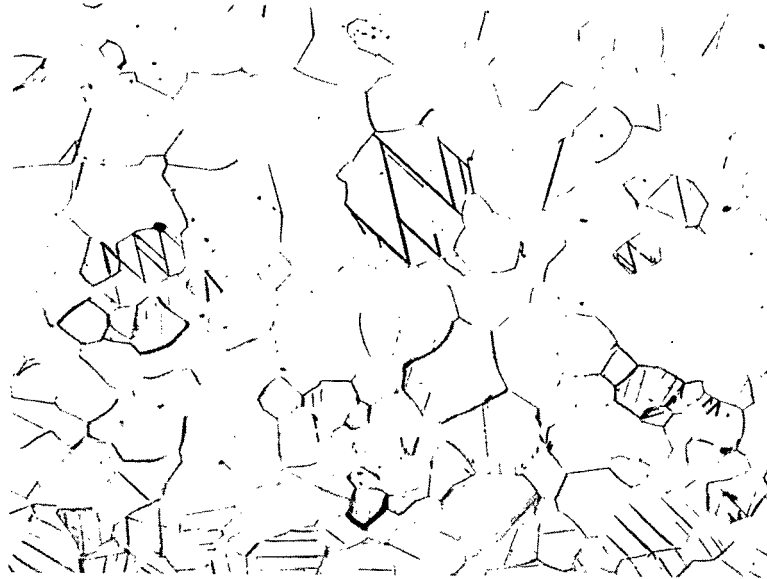
^a Measured on unstrained portion of specimen after test.

^b Step-temperature creep test.

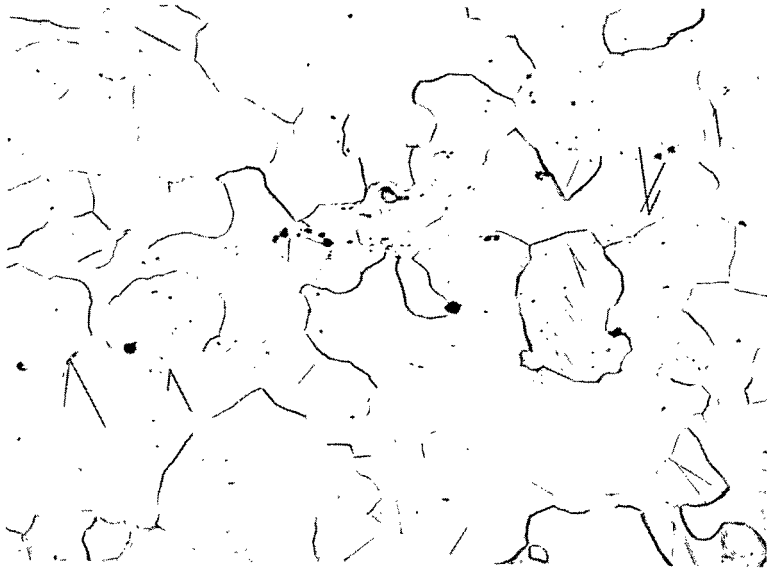
^c Step-load creep test.

^d Specimen broke in grip during creep-rupture test.

^e Test discontinued.



(a) Electron-beam-melted (EB) rhenium.



(b) Powder-metallurgy (PM) rhenium.

Figure 1. - Microstructure of rhenium sheet annealed 1 hour at 3000° F (1922 K) in hydrogen. X250.

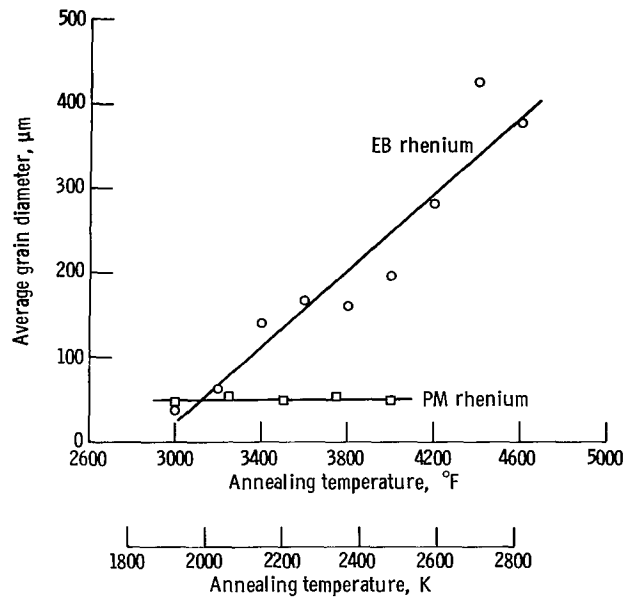
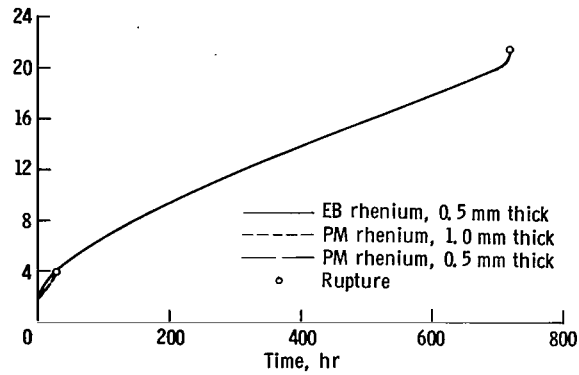
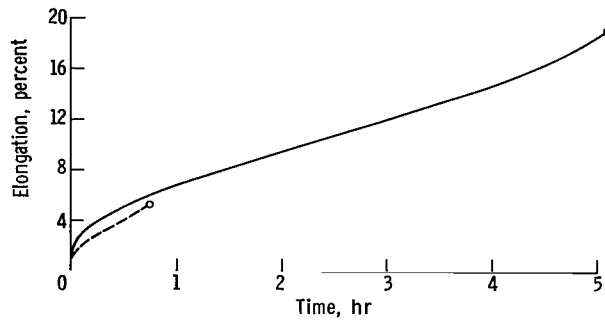


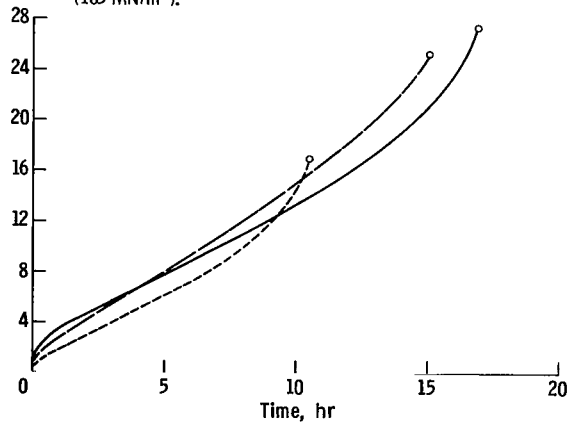
Figure 2. - Effect of 1-hour annealing temperature on grain size in electron-beam-melted (EB) and powder-metallurgy (PM) rhenium sheet.



(a) Test temperature, 2200° F (1477 K); load stress, 20 ksi (138 MN/m²).

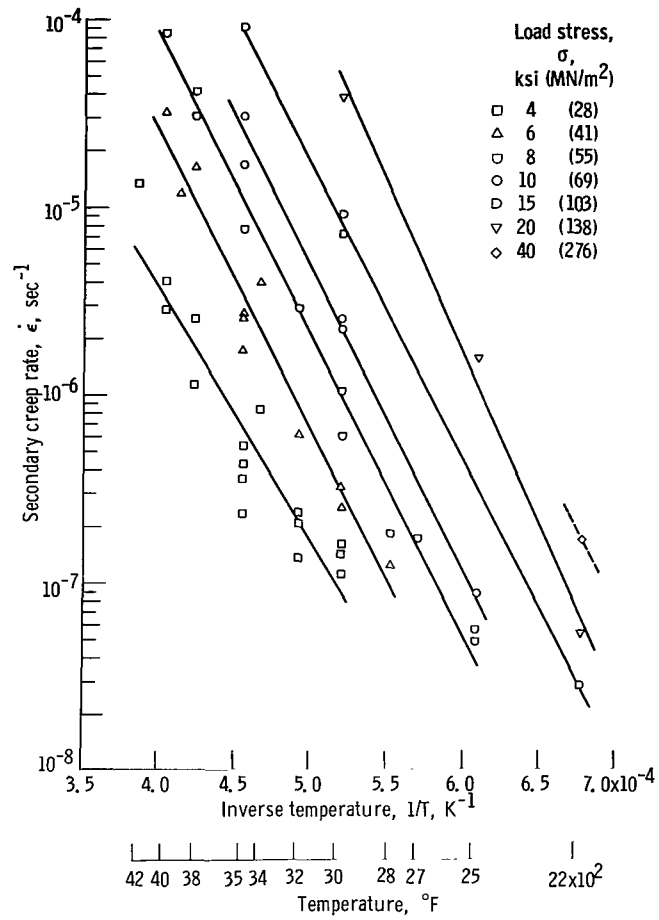


(b) Test temperature, 3000° F (1922 K); load stress, 15 ksi (103 MN/m²).



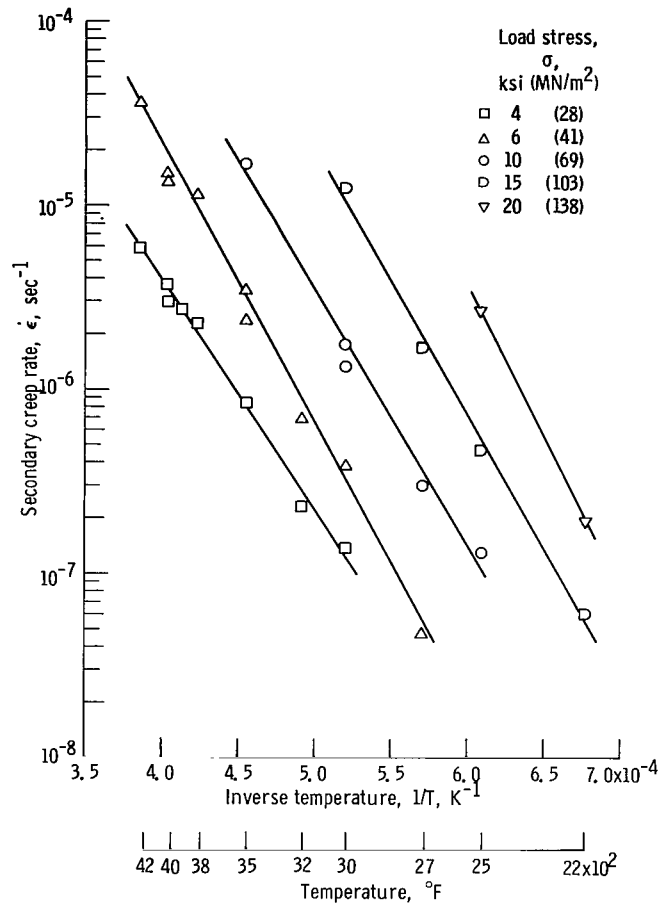
(c) Test temperature, 4000° F (2477 K); load stress, 4 ksi (28 MN/m²).

Figure 3. - Creep curves for electron-beam-melted (EB) and powder-metallurgy (PM) rhenium under various temperature and stress conditions.



(a) Electron-beam-melted rhenium sheet.

Figure 4. - Temperature dependence of secondary creep rate in rhenium for constant load stresses of 4 to 40 ksi (28 to 276 MN/m^2).



(b) Powder-metallurgy rhenium sheet

Figure 4. - Concluded.

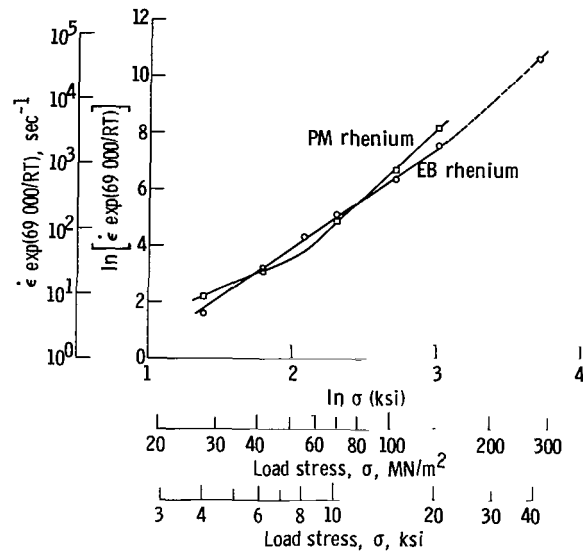


Figure 5. - Stress dependency of temperature-compensated secondary creep rate for recrystallized electron-beam-melted (EB) and powder-metallurgy (PM) rhenium.

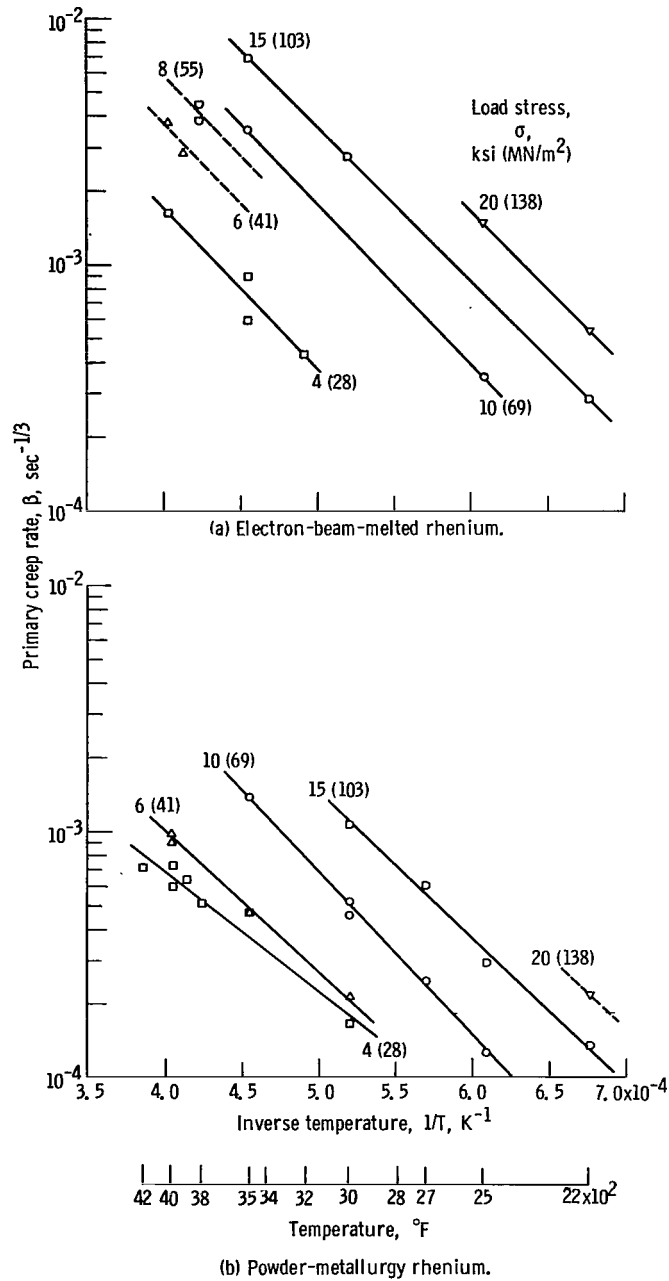


Figure 6. - Temperature dependency of primary creep rates of rhenium sheet at stresses of 4 to 20 ksi (28 to 138 MN/m^2).

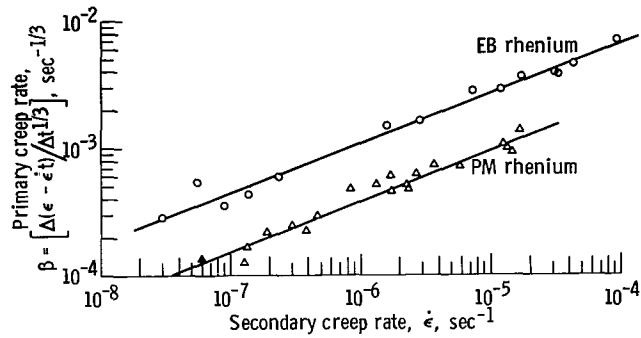


Figure 7. - Relation of primary and secondary creep rates of electron-beam-melted (EB) and powder-metallurgy (PM) rhenium at 2400° to 4200° F (1477 to 2588 K). $\beta = k(\dot{\epsilon})^{0.40}$.

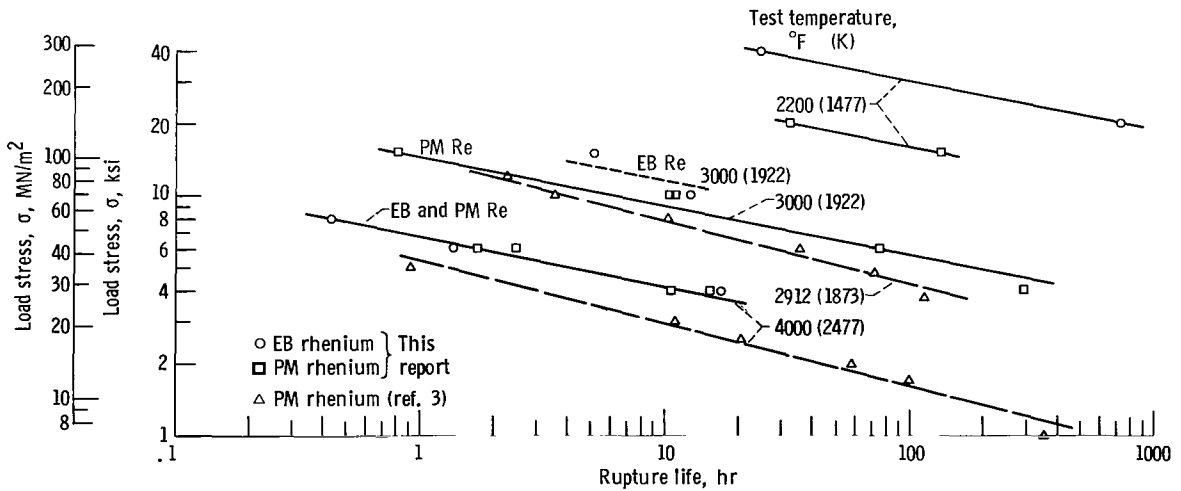
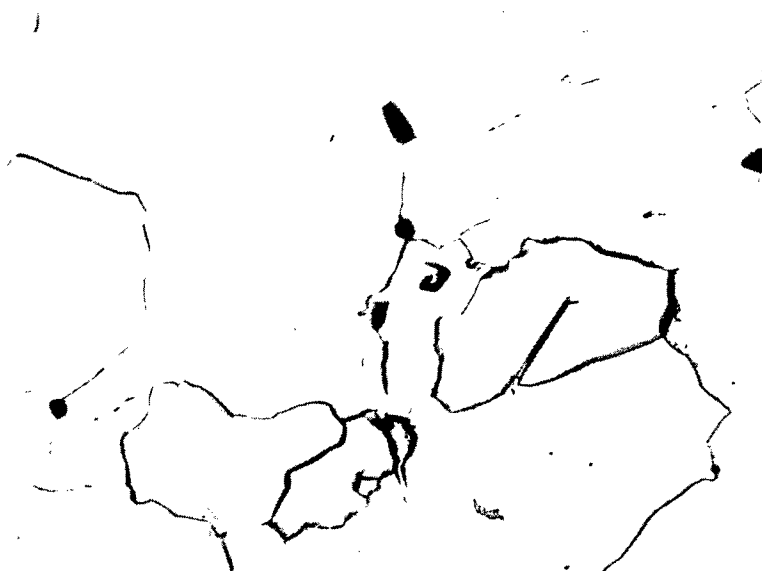


Figure 8. - Effect of creep stress on rupture life at constant temperature for electron-beam-melted (EB) and powder-metallurgy (PM) rhenium sheet at three temperature levels.



(a) Electron-beam-melted (EB) rhenium after 9 percent total elongation (broke in grip).



(b) Powder-metallurgy (PM) rhenium after 2 percent total elongation (rupture).

Figure 9. - Voids in microstructure following creep at 2500° F (1644 K) and 20 ksi 138 MN/m². X500.

NATIONAL AERONAUTICS AND SPACE ADMINISTRATION
WASHINGTON, D. C. 20546

OFFICIAL BUSINESS
PENALTY FOR PRIVATE USE \$300

FIRST CLASS MAIL



POSTAGE AND FEES PAID
NATIONAL AERONAUTICS AND
SPACE ADMINISTRATION

01U 001 42 51 3DS 71.10 00903
AIR FORCE WEAPONS LABORATORY /WL0L/
KIRTLAND AFB, NEW MEXICO 87117

ATT E. LOU BOWMAN, CHIEF, TECH. LIBRARY

POSTMASTER: If Undeliverable (Section 158
Postal Manual) Do Not Return

"The aeronautical and space activities of the United States shall be conducted so as to contribute . . . to the expansion of human knowledge of phenomena in the atmosphere and space. The Administration shall provide for the widest practicable and appropriate dissemination of information concerning its activities and the results thereof."

— NATIONAL AERONAUTICS AND SPACE ACT OF 1958

NASA SCIENTIFIC AND TECHNICAL PUBLICATIONS

TECHNICAL REPORTS: Scientific and technical information considered important, complete, and a lasting contribution to existing knowledge.

TECHNICAL NOTES: Information less broad in scope but nevertheless of importance as a contribution to existing knowledge.

TECHNICAL MEMORANDUMS: Information receiving limited distribution because of preliminary data, security classification, or other reasons.

CONTRACTOR REPORTS: Scientific and technical information generated under a NASA contract or grant and considered an important contribution to existing knowledge.

TECHNICAL TRANSLATIONS: Information published in a foreign language considered to merit NASA distribution in English.

SPECIAL PUBLICATIONS: Information derived from or of value to NASA activities. Publications include conference proceedings, monographs, data compilations, handbooks, sourcebooks, and special bibliographies.

TECHNOLOGY UTILIZATION PUBLICATIONS: Information on technology used by NASA that may be of particular interest in commercial and other non-aerospace applications. Publications include Tech Briefs, Technology Utilization Reports and Technology Surveys.

Details on the availability of these publications may be obtained from:

**SCIENTIFIC AND TECHNICAL INFORMATION OFFICE
NATIONAL AERONAUTICS AND SPACE ADMINISTRATION
Washington, D.C. 20546**